

Alma Mater Studiorum Università di Bologna
Archivio istituzionale della ricerca

Effect of lower-limb joint models on subject-specific musculoskeletal models and simulations of daily motor activities

This is the final peer-reviewed author's accepted manuscript (postprint) of the following publication:

Published Version:

Valente, G., Pitto, L., Stagni, R., Taddei, F. (2015). Effect of lower-limb joint models on subject-specific musculoskeletal models and simulations of daily motor activities. JOURNAL OF BIOMECHANICS, 48(16), 4198-4205 [10.1016/j.jbiomech.2015.09.042].

Availability:

This version is available at: <https://hdl.handle.net/11585/545202> since: 2016-06-29

Published:

DOI: <http://doi.org/10.1016/j.jbiomech.2015.09.042>

Terms of use:

Some rights reserved. The terms and conditions for the reuse of this version of the manuscript are specified in the publishing policy. For all terms of use and more information see the publisher's website.

This item was downloaded from IRIS Università di Bologna (<https://cris.unibo.it/>).
When citing, please refer to the published version.

(Article begins on next page)

This is the final peer-reviewed accepted manuscript of:

*Giordano Valente, Lorenzo Pitto, Rita Stagni, Fulvia Taddei, **Effect of lower-limb joint models on subject-specific musculoskeletal models and simulations of daily motor activities**, Journal of Biomechanics, Volume 48, Issue 16, 2015, Pages 4198-4205, ISSN 0021-9290*

The final published version is available online at:

<https://doi.org/10.1016/j.jbiomech.2015.09.042>

Rights / License:

The terms and conditions for the reuse of this version of the manuscript are specified in the publishing policy. For all terms of use and more information see the publisher's website.

This item was downloaded from IRIS Università di Bologna (<https://cris.unibo.it/>)

When citing, please refer to the published version.

Effect of lower-limb joint models on subject-specific musculoskeletal models and simulations of daily motor activities

Giordano Valente^{1*}, Lorenzo Pitto¹, Rita Stagni², Fulvia Taddei¹

1. Medical Technology Laboratory, Rizzoli Orthopaedic Institute, Bologna, Italy

2. Department of Electric, Electronic and Information Engineering, University of Bologna, Bologna, Italy

Word Count: 3660

*CORRESPONDING AUTHOR:

Giordano Valente

Laboratorio di Tecnologia Medica

Istituto Ortopedico Rizzoli

via di Barbiano 1/10, 40136 - Bologna, Italy

Phone: +39 051 6366554

e-mail: valente@tecno.ior.it

1 **ABSTRACT**

2 Understanding the validity of using musculoskeletal models is critical, making important
3 to assess how model parameters affect predictions. In particular, different joint models in
4 the articulated linkage can affect predictions from simulations of movement, and the
5 identification of image-based joints is unavoidably affected by uncertainty that can
6 potentially decrease the benefits of increasing model complexity. The aim of this study is
7 to evaluate the effect of different lower-limb joint models on muscle and joint contact
8 forces during four motor tasks, and assess the sensitivity to the uncertainties in the
9 identification of anatomical four-bar-linkage joints. Three MRI-based musculoskeletal
10 models having different knee and ankle joint models were created and used for
11 simulations of walking, chair rise, stair ascent and descent. Model predictions were
12 compared against a baseline model including simpler and widely-adopted joints. In
13 addition, a probabilistic analysis was performed by perturbing four-bar-linkage joint
14 parameters according to their uncertainty. Our findings do not support the need for knee
15 and ankle models more complex than typical hinges, as the differences in joint contact
16 forces, although dependent on the motor task analyzed, were generally not substantial.
17 However, the model including more degrees of freedom showed larger differences and
18 more discrepancies in predicted muscle activations compared to measured muscle
19 activity. Further, including image-based four-bar-linkages was robust to simulate
20 walking, chair rise and stair ascent, but not stair descent, suggesting that joint model
21 complexity should be set according to the imaging dataset available and the intended
22 application, performing sensitivity analyses.

1 **KEYWORDS**

2 Subject-specific musculoskeletal modeling, Lower-limb joint models, MRI, Four-bar-
3 linkage, Joint contact forces

4

5

6

7

8

9

10

11

12

13

14

15

1 INTRODUCTION

2 Musculoskeletal modeling and dynamic simulations of movement have a great potential
3 to give insights into musculoskeletal disorders (Arnold and Delp, 2004; Fregly et al.,
4 2012b), and there has been a growing expansion of musculoskeletal modeling
5 applications. In this context, subject-specific models provide more accurate results
6 compared to scaled-generic models (Correa et al., 2012; Lenaerts et al., 2009). Two
7 major challenges are related to the use of subject-specific models: model creation and
8 validation of model predictions. Model creation can be effort-intensive and involves
9 identification of several parameters affected by uncertainties (Valente et al., 2014).
10 Validation of muscle and joint force predictions is markedly limited (Hicks et al., 2015).
11 Therefore, sensitivity analyses have been performed to increase model reliability by
12 assessing how model parameters affect predictions (Ackland et al., 2012; Martelli et al.,
13 2015; Valente et al., 2014).

14 In particular, the assumptions that lead to specific kinematics joint models in the
15 articulated linkage affect predictions of muscle and joint contact forces during movement
16 (Dumas et al., 2012). In healthy joint conditions, while the hip can be accurately
17 modeled as a spherical joint, the knee and ankle exhibit a complex behavior (Leardini et
18 al., 2001, 1999a; Wilson et al., 2000) that have led to different modeling assumptions.
19 To describe the motion of the intact knee and ankle, one degree-of-freedom (DOF)
20 models with anatomy-based constraints (e.g., isometric ligaments, sphere-on-plane
21 contacts) have been developed that aim at reproducing physiological kinematics
22 coupling planar translations to the flexion DOF by using four-bar-linkage mechanisms
23 (Heller et al., 2007; Leardini et al., 1999b; O'Connor et al., 1989), or coupling all DOF to

flexion by using spatial parallel mechanisms (Di Gregorio et al., 2007; Feikes et al., 2003). In general, musculoskeletal models have included spherical, universal and hinge joints with or without coupled DOF at the knee and ankle (see Dumas et al., 2012 for a review). In particular, when musculoskeletal models have been used for muscle and joint force calculation, most applications have adopted simplified articulated linkages such as the widely used *Gait2392* available in OpenSim (Delp et al., 2007), or other models (Anderson and Pandy, 1999; Heller et al., 2001; Kepple et al., 1997; Modenese et al., 2011) based on *ex vivo* studies. In addition, only few models have been created from imaging data allowing capture of subject-specific anatomy to create joints with anatomy-based constraints (Correa et al., 2011; Sandholm et al., 2011; Taddei et al., 2012; Valente et al., 2014).

To date, it is not clear how different joint models affect muscle and joint forces calculated during different motor tasks using musculoskeletal models created from clinical imaging data. Particularly, the behavior of the knee and ankle joints can be markedly variable when simulating tasks having different joint ranges of motion, which leads to poses of the model that can affect dynamics outcomes. In addition, the identification of image-based joints is unavoidably affected by uncertainty due to the imaging quality available and operator variability. The introduction of more sources of uncertainty can lead to error propagation, potentially decreasing the benefits of introducing additional model complexity, and raises the questions of how complex should joints be for different musculoskeletal applications and how worth is to create more complex image-based models.

Therefore, the aim of the present study is twofold: first, to evaluate the effect of different knee and ankle joint models on muscle and joint contact forces during walking, chair rise, stair ascent and descent, by using musculoskeletal models created from lower-body MRI of a healthy subject; second, to analyze the sensitivity of muscle and joint contact forces to the uncertainty in the identification of anatomical four-bar-linkage joints from MRI.

To the purpose, we used a previously developed MRI-based model (Valente et al., 2014) as baseline to create three additional models with different anatomy-based knee and ankle joints. We compared the simulation results, obtained through a typical inverse dynamics and static optimization approach, against the baseline model to analyze the differences. Further, we used the uncertainty in the identification of four-bar-linkage parameters in a model, which involved locations of soft tissue landmarks, to evaluate the robustness of model predictions through a probabilistic approach.

MATERIALS AND METHODS

Experimental data

Lower-body MRI and motion analysis data were acquired from one healthy subject (male; age: 31 years; height: 183 cm; weight: 70.5 kg) who performs amateur sports two times per week, and shows normal neuromuscular control strategy (Supplementary Materials 1). The MRI data and motion analysis protocol have been described previously (Valente et al., 2014). In summary, four series of MR images were acquired by using a 1.5 T MR scanner (Intera, Koninklijke Philips N.V., The Netherlands). The subject performed 10 walking, chair rising, stair ascending and descending trials. Stair

ascending and descending were performed by using a modular staircase allowing measurement of ground reaction forces, and during chair rising the subject kept each foot in contact with a single force platform. In addition, two static postures (standing and sitting) were acquired. Three-dimensional motion analysis data were acquired by using a 6TV camera stereophotogrammetric system (SMART-D BTS, Milano, Italy), integrated with two dynamometric platforms for measurement of ground reaction forces (Bertec Corporation, USA) and 8-channel electromyography (EMG) recording system. Anatomical landmark trajectories were quantified by using an 8-segment protocol (feet, shanks, thighs, pelvis and trunk) based on the C.A.S.T. approach (Cappozzo et al., 1995), implementing double-calibration (Cappello et al., 2005) of thigh and shank landmarks. EMG activity of gluteus maximus, biceps femoris long head, semitendinosus, rectus femoris, vastus medialis, gastrocnemius, soleus and tibialis anterior was acquired at 1000 Hz sampling frequency according to SENIAM recommendations (Hermens, 2000). EMG data were high-pass filtered (10 Hz), rectified and low-pass filtered (6 Hz).

Baseline musculoskeletal model

The baseline OpenSim model used in this study has been developed from MRI and described previously (Valente et al., 2014). In summary, the model was defined as a 7-segment, 10-DOF articulated system, actuated by 84 musculotendon units. All necessary anatomical landmarks were virtually palpated on the body surfaces with the help of the superimposed MRI, to define reference frames and joint constraints. Each hip was modeled as a 3-DOF spherical joint, each knee and ankle as a 1-DOF revolute hinge joint. The hip joint was defined at the center of the femoral head, the knee and ankle axes of rotation were defined as the line connecting the landmarks identified on

the medial and lateral epicondyles and medial and lateral tips of malleoli, respectively. The number and paths of the musculotendon actuators were defined according to a generic model (Delp et al., 1990). The maximum isometric force of each musculotendon unit was estimated as the product of the muscle physiological cross-sectional area and the maximum muscle tension, assuming muscle fiber length proportional to musculotendon length (Correa and Pandy, 2011). The model was created by using the freely available NMSBuilder software (Valente et al., 2014). The baseline model will be named *Spherical – Hinge – Hinge* (SHH) hereinafter, indicating a spherical joint at the hip and a revolute hinge joint at the knee and ankle.

Modified models

Three additional OpenSim models were created based on the baseline SHH model (Fig. 1), by modifying the knee and ankle joint parameters only, and described as follows:

1. *Spherical - modified Hinge - Universal* (SH*U): same configuration of joint kinematics constraints of the widely-used *Gait2392* generic model (Delp et al., 2007). Specifically, the knee joint has one DOF with coupled planar translations (Yamaguchi and Zajac, 1989), where the plane of motion is perpendicular to the knee axis. Planar translations were expressed as functions of the knee angle, which were obtained by scaling the generic model to the subject's dimensions. The ankle complex was modeled as a 2-DOF universal joint, including two hinges at the tibiotalar and subtalar joint with non-intersecting rotational axes. The tibiotalar joint was modeled as in the baseline SHH model, the orientation and

location of the subtalar joint was identified on the MRI data according to Isman and Inman, 1969.

2. *Spherical - modified Spherical - Universal (SS*U)*: same configuration of joint kinematics constraints of a modified generic OpenSim model (Donnelly et al., 2012). Specifically, the knee has three rotational DOF with two planar translations coupled with the flexion DOF. Knee coupled translations and the ankle joint were modeled as in SH*U.

3. *Spherical - anatomical four-bar-linkage - anatomical four-bar-linkage (SH_{4BL}H_{4BL})*: the knee and ankle were modeled as a 1-DOF joint with two coupled planar translations (Leardini et al., 1999b; O'Connor et al., 1989) based on the subject-specific joint anatomy (Fig. 1). Joint ligaments, identified on the MRI and assumed isometric during motion, act as constraints to motion between the proximal and distal body segments. Specifically, in the knee mechanism, the origin and insertion points of the anterior cruciate (ACL) and posterior cruciate (PCL) ligaments were projected on the plane perpendicular to the flexion axis and passing through the mid point of the epicondyles to define a four-bar-linkage with inextensible links whose movement was constrained on the plane. Similarly, in the ankle mechanism, the origin and insertion points of the calcaneo-fibular (CaFib) and tibial-calcaneal (TiCal) ligaments were projected on the plane perpendicular to the flexion axis and passing through the mid point of the malleoli to define a four-bar-linkage with inextensible links whose movement was constrained on the plane. Joint kinematics was obtained by implementing the constraint equations (Feikes et al., 2003) based on anatomical landmarks

locations and then solving the system for the coupled planar translations. Values for the coupled planar translations at the knee and the ankle in the physiological range of flexion are reported in Supplementary Materials 2.

Simulations of motor tasks

Using the four musculoskeletal models (baseline SHH and the three modified SH*U, SS*U and SH_{4BL}H_{4BL}), simulations of a randomly selected cycle of walking, chair rise, stair ascent and descent were run leveraging OpenSim. First, joint angles were calculated through Inverse Kinematics. A global optimization problem was solved that minimized the differences between experimentally-measured marker trajectories and the corresponding markers placed on the models (Delp et al., 2007), formulated as weighted least squares problem with uniform weightings. Muscle forces and activations were calculated through Static Optimization, minimizing the sum of muscle activations squared and neglecting the force-length-velocity relationships of muscle (Anderson and Pandy, 2001). Finally, joint contact forces were calculated through Joint Reaction Analysis, solving for the dynamic equilibrium at each body segment.

Sensitivity to the identification of anatomical four-bar-linkage joints

A probabilistic analysis was performed to study the sensitivity of the SH_{4BL}H_{4BL} model to the uncertainties associated with the creation of the anatomical four-bar-linkage at the knee and ankle joints. The positions of the eight landmarks identifying the origin and insertion points of ACL, PCL, CaFib and TiCal were assumed as multivariate normally distributed variables. The distribution of each variable was calculated experimentally (Table 1; Supplementary Materials 4): four expert operators virtually palpated the

landmarks on the bone surfaces with the help of the superimposed MRI three times, by using NMSBuilder. Positions of bony landmarks (i.e., epicondyles and malleoli) identifying the orientation of the planes in which rotations and coupled translations occur were not perturbed, as previous research has demonstrated limited uncertainty associated and non-significant effect on model predictions (Martelli et al., 2015; Valente et al., 2014). A Latin Hypercube Sampling (LHS) strategy (McKay et al., 1979; Valente et al., 2013) was applied to generate an efficient sampling of input variables from their distribution. This allowed creation of OpenSim models including different knee and ankle four-bar-linkage models corresponding to each set of sampled variable values. Using each model, the same workflow for simulations of movement was re-run. Two-hundred simulations per motor task ensured convergence of the output variables (Valente et al., 2014). Static optimization simulations were considered failed (i.e., joint dynamic equilibrium not achieved) if the use of reserve actuators on any joint DOF exceeded 5% of the peak joint moment (van der Krogt et al., 2012) in at least one frame of the motor task cycle. Simulations of walking, stair ascent and chair rise were all successful, while 27% of stair descent simulations failed and were not included in the subsequent analysis.

Data Analysis

The analysis was focused on hip, knee and ankle joint contact forces, and muscle activations corresponding to measured EMG recordings. First, all quantities were expressed in percentage of the motor task cycle, and the forces were also normalized to the subject body-weight (BW).

To assess variability in model outcomes, results from the three modified models were compared against the baseline model, as the articulated linkage (SHH) of the baseline model is widely adopted and considered state-of-the-art in musculoskeletal dynamics applications. Specifically, mean and maximum differences in joint contact forces over each motor task cycle were calculated. In addition, Wilcoxon signed rank tests ($p < 0.01$) were performed to evaluate significant differences among model outcomes, and Pearson correlation coefficients (R) were calculated to quantify similarities. To qualitatively assess validity of the models, muscle activations predicted using the different models were compared against measured EMG.

To analyze the sensitivity to the uncertainties in identifying four-bar-linkage mechanisms, standard deviations (mean and maximum over each motor task cycle) of joint contact forces predicted through the perturbed SH_{4BL}H_{4BL} models were calculated for each simulated motor task.

RESULTS

Model variability

Overall, the differences in joint contact forces between the modified models and the baseline model were dependent on the motor task analyzed (Fig. 2, Table 2; Supplementary Materials 3). The SH*U and SH_{4BL}H_{4BL} models showed relatively mild differences. SH*U presented a peak in mean difference of 0.28 BW at the ankle during stair descent (maximum difference of 0.73 BW), and tended to underestimate knee loads and overestimate ankle loads (Table 2). SH_{4BL}H_{4BL} presented a peak in mean difference of 0.25 BW at the ankle during stair descent (maximum difference of 1.54

BW), and tended to overestimate hip loads, underestimate knee loads (except for walking) and not differ at the ankle (except for stair descent) (Table 2). The SS*U model showed more marked differences, with a peak in mean difference of 0.59 BW at the knee during walking (maximum difference of 2.4 BW). This model tended to overestimate all loads. High correlation values were observed between all modified models and baseline model (Table 2), confirming similarities in force patterns.

Predicted muscle activation patterns in all models were generally consistent with EMG recordings, apart from few discrepancies in tibialis anterior and hamstrings (Fig. 3). The SS*U model presented additional discrepancies in the activations of biceps femoris during walking and gastrocnemius during stair ascent and descent.

Sensitivity analysis

During walking, chair rise and stair ascent, the uncertainties in the identification of the SH_{4BL}H_{4BL} model did not have a marked effect on joint contact forces, showing mean standard deviations over the motor task cycles below 0.26 BW (Fig. 4, Table 3). Conversely, during stair descent, there was a marked effect on knee and ankle forces, showing a mean standard deviation of 0.4 BW and a maximum of 2.66 BW at the ankle.

DISCUSSION

Our goal was: first, to analyze the effect of different knee and ankle joint models on the predictions of joint contact forces during four motor tasks by using musculoskeletal models created from lower-body MRI; and second, to evaluate how sensitive are predictions to the uncertainties in the identification of four-bar-linkage joint parameters

1 from the data available. When routine clinical images are available, our results do not
2 support the need for knee and ankle models more complex than typical hinges, and
3 suggest that the model including anatomical knee and ankle four-bar-linkage joints
4 ($SH_{4BL}H_{4BL}$) is robust to simulate walking, chair rise and stair ascent, but not stair
5 descent.

6 Comparing the joint contact forces predicted by using the three modified models
7 (including different knee and ankle kinematics constraints) and the baseline model
8 (including simpler and widely-used joint constraints), we found differences that were
9 generally not substantial, and the predicted forces presented marked similarities in
10 patterns (Fig. 2, Table 2). In fact, the maximum mean differences over the motor task
11 cycle were 0.59 BW in overestimation and -0.21 BW in underestimation, and the high
12 correlation coefficients indicated a good correspondence in force changes over the
13 motor task cycle. However, the SS*U model presented larger differences that could
14 reach notable maximum values (2.4 BW at the knee during walking). Comparing
15 predicted muscle activity to measured EMG allowed to identify SS*U as the least
16 accurate model, as more discrepancies in muscle onset/offset timing were shown.
17 However, we were not able to discriminate which model performed best, as this indirect
18 validation method does not allow a direct comparison. A given modified model
19 compared to the baseline could overestimate, underestimate or present no significant
20 differences depending on the task analyzed. Particularly, adding more DOF at the knee
21 (SS*U) caused an overall overestimation of the loads due to an increase in quadriceps
22 muscle forces (Figs. 2 and 3) that had to compensate for additional joint moments.
23 Conversely, including more physiological constraints at the knee (SH^*U and $SH_{4BL}H_{4BL}$)

caused underestimation of the loads when an increase in quadriceps muscle moment arms reduced the required force to equilibrate joint moments. The inclusion of a 2-DOF joint at the ankle (SH*U and SS*U) led to a general increase in ankle loads, while more physiological joint constraints at the ankle (SH_{4BL}H_{4BL}) caused no significant differences apart from stair descent where decreased moment arms of plantarflexor muscles required more forces from those muscles.

Analyzing the sensitivity of joint contact forces to the uncertainties in the identification of knee and ankle four-bar-linkage mechanisms (SH_{4BL}H_{4BL}), we found a moderate effect during walking, chair rise and stair ascent, showing a maximum standard deviation of 0.66 BW at the ankle during stair ascent (Fig. 4, Table 3). Conversely, we found a more marked sensitivity of knee and ankle forces during stair descent. Notably, the late stance phase showed a maximum standard deviation of 1.21 BW and 2.66 BW at the knee and ankle force, respectively, in conjunction with unrealistic peak magnitude at the ankle (up to 13 BW). In this situation, the joint contact forces were more sensitive to changes in joint kinematics, particularly to the planar translations coupled to ankle dorsiflexion, which decreased the moment arms of gastrocnemii and soleus. This produced a sensitive increase in the forces exerted by those muscles, leading in turn to sensitive increases in ankle forces that propagated to the knee. We did not analyze the uncertainties in the identification of the other joint models (SHH, SH*U, SS*U), as this involves identification of few bony landmarks only, and it has been previously demonstrated not to have a significant effect on force predictions (Martelli et al., 2015; Valente et al., 2014).

As reported in previous literature (Dumas et al., 2012; Glitsch and Baumann, 1997; Mokhtarzadeh et al., 2014), we found an overall increase in joint contact forces when increasing the number of DOF in the model (SS*U). In this scenario, we confirmed a decrease in soleus activity (Mokhtarzadeh et al., 2014) when using a 3-DOF knee model and the same static optimization method, although different tasks were simulated. However, in contrast to Dumas et al., 2012, we found an increase in vasti and gastrocnemius activity when using a 3-DOF knee model during walking, which led to an increase in both knee force peaks. In this case, a different subject's kinematics recorded and the inclusion of subject-specific anatomical detail in the model may have affected the different result of muscle coordination strategy.

Our findings should be evaluated under the light of some limitations. First, we created the musculoskeletal models from data of one subject only. Inter-subject variability in bone and soft tissue anatomy might influence the effect of the implemented joint models on force predictions. In particular, measures of passive joint laxity of the subject would have provided additional understanding of the physiological context where our findings hold; however, we reported the calculated translations at the knee and ankle in the four-bar-linkage model and quantified the neuromotor control strategy of the subject. Further, we compared the effect of a limited set of knee and ankle joint models without including other anatomical joints (Di Gregorio et al., 2007; Feikes et al., 2003) that could have potentially led to different results. However, we intended to analyze the most common joint modeling choices for musculoskeletal modeling applications. In addition, we used a limited dataset that was not optimized for specific joint modeling purposes such as the "Grand Challenge Competition to predict *in vivo* knee loads" (Fregly et al., 2012a), but

1 was representative of typical clinical routine activities, which allowed us to simulate real
2 scenarios of patient-specific modeling from clinical imaging.

3 The findings of our study suggest that knee and ankle model complexity in
4 musculoskeletal models should be set according to the dataset details available.
5 Particularly, MRI acquired for diagnostic purposes to obtain a general overview of bone
6 and soft tissues may provide accurate identification of origin and insertion of knee and
7 ankle ligaments used to create anatomical joints. However, there could be cases where
8 model robustness is not acceptable for the specific application, as stair descent
9 simulations demonstrated in this study. Therefore, sensitivity analyses to parameter
10 uncertainties are suggested before using a more complex model, and care should be
11 taken when evaluating calculated forces according to the intended application,
12 particularly in correspondence of the peaks of knee and ankle loads, where variability
13 could be higher.

14 In summary, our study revealed that when using routine clinical imaging to create
15 musculoskeletal models of healthy young subjects with normal neuromotor control
16 strategy and no relevant degree of dynamic joint laxity, there is no need to implement
17 knee and ankle models more complex than typical hinges, and the effect of using
18 kinematic models including coupled translational degrees of freedom would be minimal.
19 In addition, including anatomical four-bar-linkage joints is robust during most tasks
20 simulated, but, in general, sensitivity analyses to joint parameter uncertainties are
21 suggested according to the dataset available and motor task to simulate. Finally, care is
22 suggested when evaluating force predictions according to the intended application, as in

many clinical applications it is impossible to discriminate which model produces the most accurate predictions.

CONFLICT OF INTEREST STATEMENT

The authors do not have any financial or personal relationships with other people or organization that could inappropriately influence their work.

ACKNOWLEDGEMENTS

This study was funded in part by the EU-funded NMS Physiome project (FP7-ICT-248189).

REFERENCES

Ackland, D.C., Lin, Y.-C., Pandy, M.G., 2012. Sensitivity of model predictions of muscle function to changes in moment arms and muscle–tendon properties: A Monte-Carlo analysis. *Journal of Biomechanics* 45, 1463–1471.

Anderson, F.C., Pandy, M.G., 1999. A Dynamic Optimization Solution for Vertical Jumping in Three Dimensions. *Computer Methods in Biomechanics and Biomedical Engineering* 2, 201–231.

Anderson, F.C., Pandy, M.G., 2001. Static and dynamic optimization solutions for gait are practically equivalent. *Journal of Biomechanics* 34, 153–161.

Arnold, A.S., Delp, S.L., 2004. The role of musculoskeletal models in patient assessment and treatment. In: Gage, J.R. (Ed.), *Treatment of Gait Problems in Cerebral Palsy*. Cambridge Press, pp. 163–177.

- 1 Cappello, A., Stagni, R., Fantozzi, S., Leardini, A., 2005. Soft Tissue Artifact
2 Compensation in Knee Kinematics by Double Anatomical Landmark Calibration :
3 Performance of a Novel Method During Selected Motor Tasks. IEEE Transactions
4 on Biomedical Engineering 52, 992–998.
- 5 Cappozzo, a, Catani, F., Croce, U. Della, Leardini, A., 1995. Position and orientation in
6 space of bones during movement: anatomical frame definition and determination.
7 Clinical Biomechanics (Bristol, Avon) 10, 171–178.
- 8 Correa, T.A., Pandy, M.G., 2011. A mass-length scaling law for modeling muscle
9 strength in the lower limb. Journal of Biomechanics 44, 2782–2789.
- 10 Correa, T.A., Schache, A.G., Graham, H.K., Baker, R., Thomason, P., Pandy, M.G.,
11 2012. Potential of lower-limb muscles to accelerate the body during cerebral palsy
12 gait. Gait & Posture 36, 194–200.
- 13 Correa, T.A., Baker, R., Graham, H.K., Pandy, M.G., 2011. Accuracy of generic
14 musculoskeletal models in predicting the functional roles of muscles in human gait.
15 Journal of Biomechanics 44, 2096–2105.
- 16 Delp, S.L., Anderson, F.C., Arnold, A.S., Loan, P., Habib, A., John, C.T., Guendelman,
17 E., Thelen, D.G., 2007. OpenSim: open-source software to create and analyze
18 dynamic simulations of movement. IEEE Transactions on Biomedical Engineering
19 54, 1940–1950.

1 Delp, S.L., Loan, J.P., Hoy, M.G., Zajac, F.E., Topp, E.L., Rosen, J.M., 1990. An
2 interactive graphics-based model of the lower extremity to study orthopaedic
3 surgical procedures. *IEEE Transactions on Biomedical Engineering* 37, 757–767.

4 Di Gregorio, R., Parenti-Castelli, V., O'Connor, J.J., Leardini, A., 2007. Mathematical
5 models of passive motion at the human ankle joint by equivalent spatial parallel
6 mechanisms. *Medical & Biological Engineering & Computing* 45, 305–313.

7 Donnelly, C.J., Lloyd, D.G., Elliott, B.C., Reinbolt, J.A., 2012. Optimizing whole-body
8 kinematics to minimize valgus knee loading during sidestepping: implications for
9 ACL injury risk. *Journal of Biomechanics* 45, 1491–1497.

10 Dumas, R., Moissenet, F., Gasparutto, X., Cheze, L., 2012. Influence of joint models on
11 lower-limb musculo-tendon forces and three-dimensional joint reaction forces during
12 gait. *Proceedings of the Institution of Mechanical Engineers, Part H: Journal of*
13 *Engineering in Medicine* 226, 146–160.

14 Feikes, J.D., O'Connor, J.J., Zavatsky, A.B., 2003. A constraint-based approach to
15 modelling the mobility of the human knee joint. *Journal of Biomechanics* 36, 125–
16 129.

17 Fregly, B.J., Besier, T.F., Lloyd, D.G., Delp, S.L., Banks, S.A., Pandy, M.G., Lima,
18 D.D.D., 2012a. Grand Challenge Competition to Predict In Vivo Knee Loads.
19 *Journal of Orthopaedic Research* 30, 503–513.

20 Fregly, B.J., Boninger, M.L., Reinkensmeyer, D.J., 2012b. Personalized
21 neuromusculoskeletal modeling to improve treatment of mobility impairments: a

perspective from European research sites. *Journal of NeuroEngineering and Rehabilitation* 9, 18.

Glitsch, U., Baumann, W., 1997. The three-dimensional determination of internal loads in the lower extremity. *Journal of Biomechanics* 30, 1123–1131.

Heller, M.O., Bergmann, G., Deuretzbacher, G., Dürselen, L., Pohl, M., Claes, L., Haas, N.P., Duda, G.N., 2001. Musculo-skeletal loading conditions at the hip during walking and stair climbing. *Journal of Biomechanics* 34, 883–893.

Heller, M.O., König, C., Graichen, H., Hinterwimmer, S., Ehrig, R.M., Duda, G.N., Taylor, W.R., 2007. A new model to predict in vivo human knee kinematics under physiological-like muscle activation. *Journal of Biomechanics* 40, S45–S53.

Hermens, H.J., Freriks, B., Disselhorst-Klug, C., Rau, G., 2000. Development of recommendations for SEMG sensors and sensor placement procedures. *Journal of Electromyography and Kinesiology* 10, 361–374.

Hicks, J.L., Uchida, T.K., Seth, A., Rajagopal, A., Delp, S.L., 2015. Is my model good enough? Best practices for verification and validation of musculoskeletal models and simulations of human movement. *Journal of Biomechanical Engineering* 137, 020905

Isman, R.E., Inman, V.T., 1969. Anthropometric Studies of the Human Foot and Ankle. *Foot Ankle. Bulletin of Prosthetics Research* 11, 97-129.

1 Kepple, T.M., Siegel, K.L., Stanhope, S.J., 1997. Relative contributions of the lower
2 extremity joint moments to forward progression and support during gait. *Gait &*
3 *Posture* 6, 1–8.

4 Leardini, A., O'Connor, J.J., Catani, F., Giannini, S., 1999a. Kinematics of the human
5 ankle complex in passive flexion; a single degree of freedom system. *Journal of*
6 *Biomechanics* 32, 111–118.

7 Leardini, A., O'Connor, J.J., Catani, F., Giannini, S., 1999b. A geometric model of the
8 human ankle joint. *Journal of Biomechanics*. 32, 585–591.

9 Leardini, A., Stagni, R., O'Connor, J.J., 2001. Mobility of the subtalar joint in the intact
10 ankle complex. *Journal of Biomechanics* 34, 805–809.

11 Lenaerts, G., Bartels, W., Gelaude, F., Mulier, M., Spaepen, A., Van der Perre, G.,
12 Jonkers, I., 2009. Subject-specific hip geometry and hip joint centre location affects
13 calculated contact forces at the hip during gait. *Journal of Biomechanics* 42, 1246–
14 1251.

15 Martelli, S., Valente, G., Viceconti, M., Taddei, F., 2015. Sensitivity of a subject-specific
16 musculoskeletal model to the uncertainties on the joint axes location. *Computer*
17 *Methods in Biomechanics and Biomedical Engineering* 18, 1555–1563.

18 McKay, M.D., Beckman, R.J., Conover, W.J., 1979. Comparison of Three Methods for
19 Selecting Values of Input Variables in the Analysis of Output from a Computer
20 Code. *Technometrics* 21, 239–245.

- 1 Modenese, L., Phillips, A.T.M., Bull, A.M.J., 2011. An open source lower limb model: Hip
2 joint validation. *Journal of Biomechanics* 44, 2185–2193.
- 3 Mokhtarzadeh, H., Perraton, L., Fok, L., Muñoz, M.A., Clark, R., Pivonka, P., Bryant,
4 A.L., 2014. A comparison of optimisation methods and knee joint degrees of
5 freedom on muscle force predictions during single-leg hop landings. *Journal of*
6 *Biomechanics* 47, 2863–2868.
- 7 O'Connor, J.J., Shercliff, T.L., Biden, E., Goodfellow, J.W., 1989. The Geometry of the
8 Knee in the Sagittal Plane. *Proceedings of the Institution of Mechanical Engineers,*
9 *Part H: Journal of Engineering in Medicine* 203, 223–233.
- 10 Sandholm, A., Schwartz, C., Pronost, N., Zee, M., Voigt, M., Thalmann, D., 2011.
11 Evaluation of a geometry-based knee joint compared to a planar knee joint. *The*
12 *Visual Computer* 27, 161-171.
- 13 Taddei, F., Martelli, S., Valente, G., Leardini, A., Benedetti, M.G., Manfrini, M., Viceconti,
14 M., 2012. Femoral loads during gait in a patient with massive skeletal
15 reconstruction. *Clinical Biomechanics (Bristol, Avon)* 27, 273–280.
- 16 Valente, G., Pitto, L., Testi, D., Seth, A., Delp, S.L., Stagni, R., Viceconti, M., Taddei, F.,
17 2014. Are Subject-Specific Musculoskeletal Models Robust to the Uncertainties in
18 Parameter Identification? *PLoS One* 9, e112625.
- 19 Valente, G., Taddei, F., Jonkers, I., 2013. Influence of weak hip abductor muscles on
20 joint contact forces during normal walking: probabilistic modeling analysis. *Journal*
21 *of Biomechanics* 46, 2186–2193.

- 1 van der Krogt, M.M., Delp, S.L., Schwartz, M.H., 2012. How robust is human gait to
2 muscle weakness? *Gait & Posture* 36, 113-119.
- 3 Wilson, D.R., Feikes, J.D., Zavatsky, a B., O'Connor, J.J., 2000. The components of
4 passive knee movement are coupled to flexion angle. *Journal of Biomechanics* 33,
5 465–473.
- 6 Wu, G., Siegler, S., Allard, P., Kirtley, C., Leardini, A., Rosenbaum, D., Whittle, M.,
7 D'Lima, D.D., Cristofolini, L., Witte, H., Schmid, O., Stokes, I., 2002. ISB
8 recommendation on definitions of joint coordinate system of various joints for the
9 reporting of human joint motion--part I: ankle, hip, and spine. International Society
10 of Biomechanics. *Journal of Biomechanics* 35, 543–548.
- 11 Yamaguchi, G.T., Zajac, F.E., 1989. A planar model of the knee joint to characterize the
12 knee extensor mechanism. *Journal of Biomechanics* 22, 1–10.

Figure 1. Definition of the joint constraints in the articulated linkages of the subject-specific musculoskeletal models used in this study: baseline SHH model (simple state-of-the-art articulated linkage (Valente et al., 2014)) and the three modified SH*U (same articulated linkage of the generic *Gait2392* model (Delp et al., 2007)), SS*U (same articulated linkage of a modified generic model (Donnelly et al., 2012)) and SH_{4BL}H_{4BL} (articulated linkage with anatomy-based four-bar-linkage at the knee and ankle) models. The anatomical four-bar-linkage joints in the SH_{4BL}H_{4BL} model were defined as planar mechanisms whose motion is constrained by joint ligaments (ACL and PCL in the knee; CaFib and TiCal in the ankle).

Figure 2. Lower-limb joint contact forces in body-weight (BW), predicted by using the baseline model (SHH) and the modified models (SH*U, SS*U, SH_{4BL}H_{4BL}) during the four motor tasks simulated.

Figure 3. Muscle activations predicted by using the baseline model (SHH) and the modified models (SH*U, SS*U, SH_{4BL}H_{4BL}), and experimental EMG activities during the four motor tasks. EMG activities are normalized to the peaks of muscle activation over the motor task cycle.

Figure 4. Lower-limb joint contact forces in body-weight (BW), predicted by using the baseline SHH model and the set of perturbed SH_{4BL}H_{4BL} models (± 1 standard deviation) during the four motor tasks simulated.

Supplementary Materials 1. Neuromuscular control strategy of the subject. Co-contraction indexes of different antagonistic muscles during the different motor tasks.

Supplementary Materials 2. Knee and ankle planar translations coupled with the flexion degree of freedom in the SH_{4BL}H_{4BL} model. Mean (solid line) and standard deviation (band) from the perturbed point locations of the antero-posterior and cranio-caudal translations plotted against the physiological range of joint flexion.

Supplementary Materials 3. Lower-limb joint kinematics, predicted by using the baseline model (SHH), the modified models (SH*U, SS*U, SH_{4BL}H_{4BL}) and the set of perturbed SH_{4BL}H_{4BL} models (± 1 standard deviation) during the four motor tasks simulated.

Supplementary Materials 4. Coordinates of the perturbed landmark points with respect to the corresponding body reference frame. Four operators virtually palpated the landmark points on the body surfaces with the help of the superimposed MRI three times.

Figure 1
[Click here to download high resolution image](#)

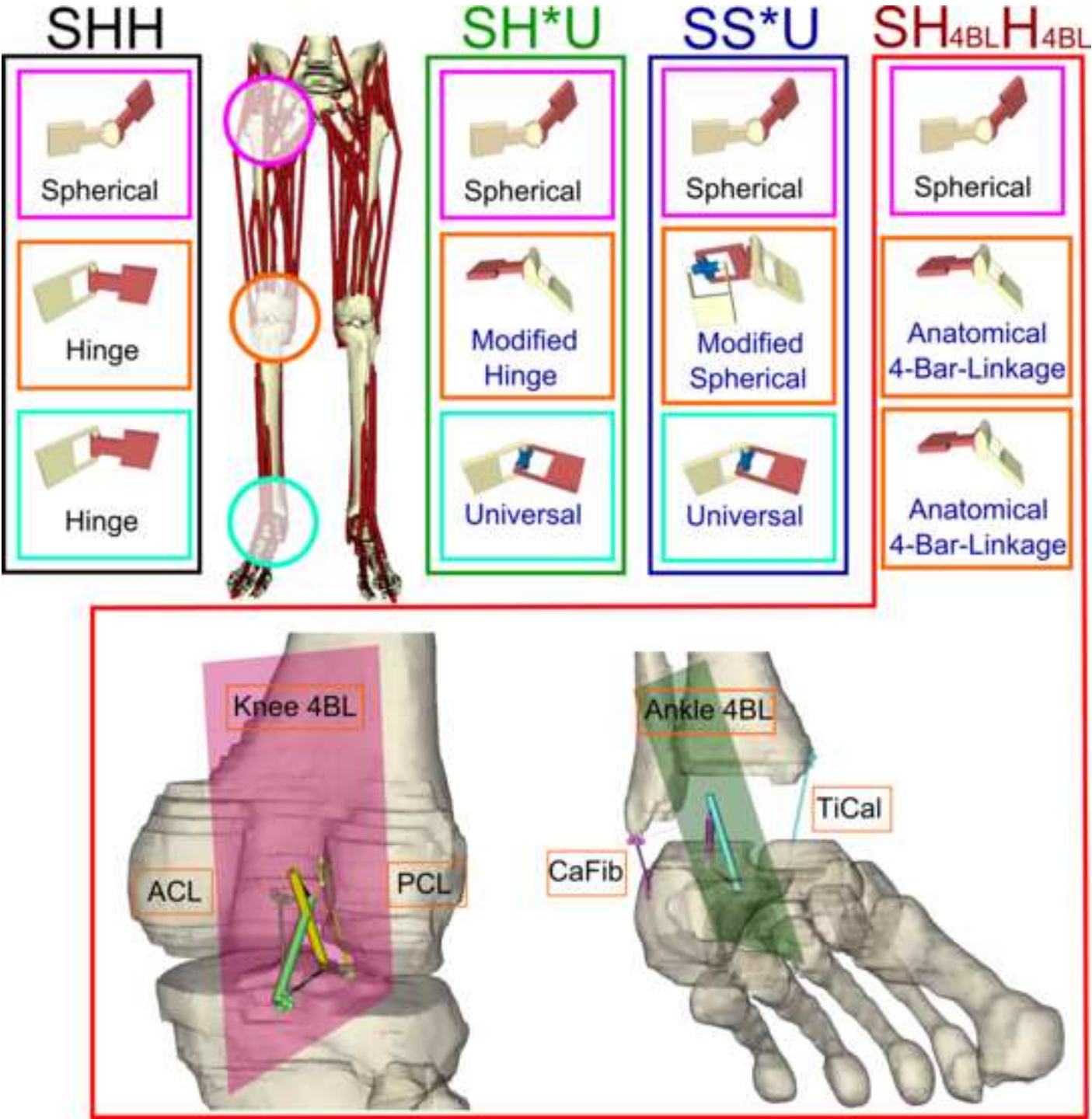


Figure 2
[Click here to download high resolution image](#)

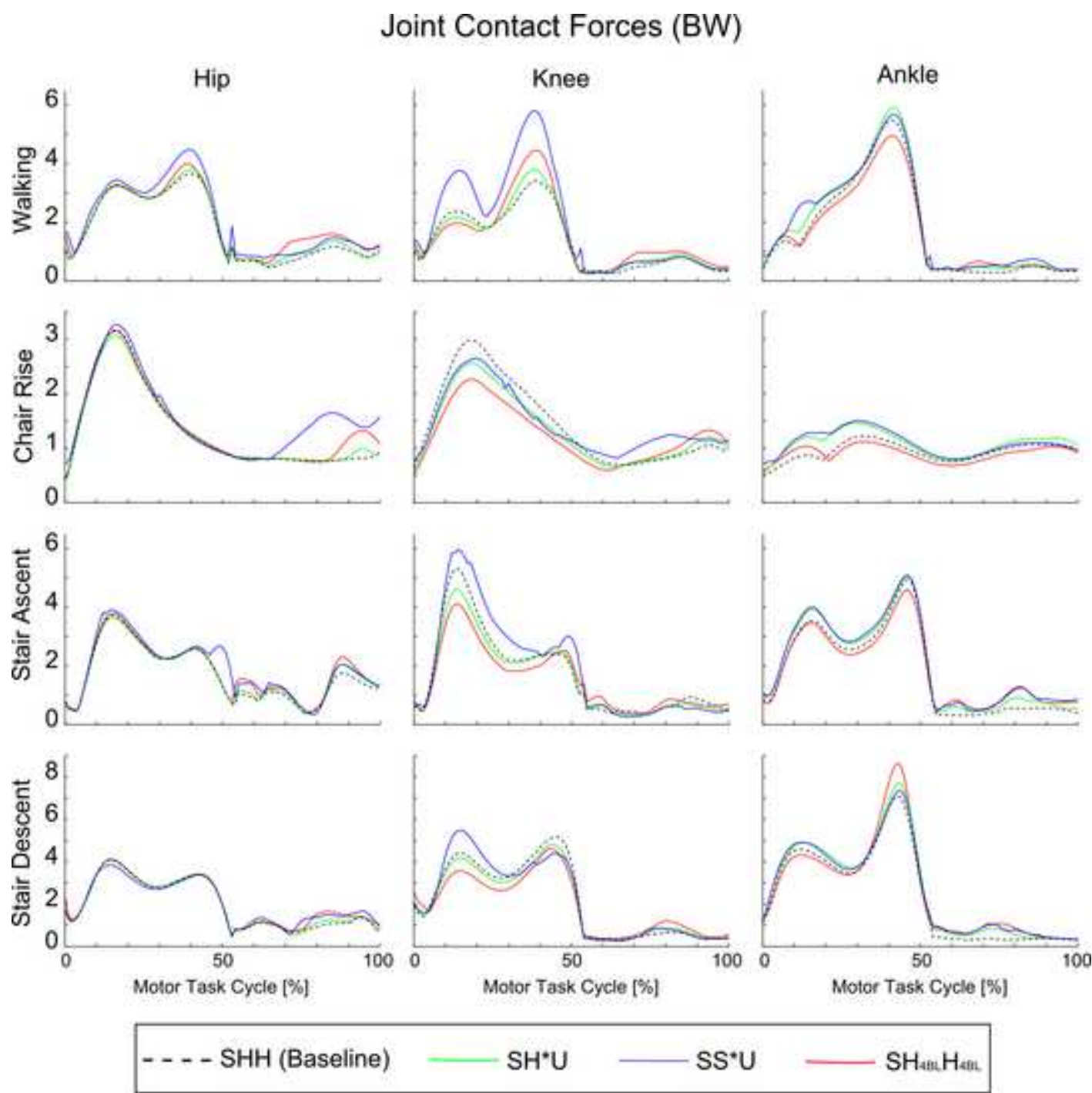


Figure 3
[Click here to download high resolution image](#)

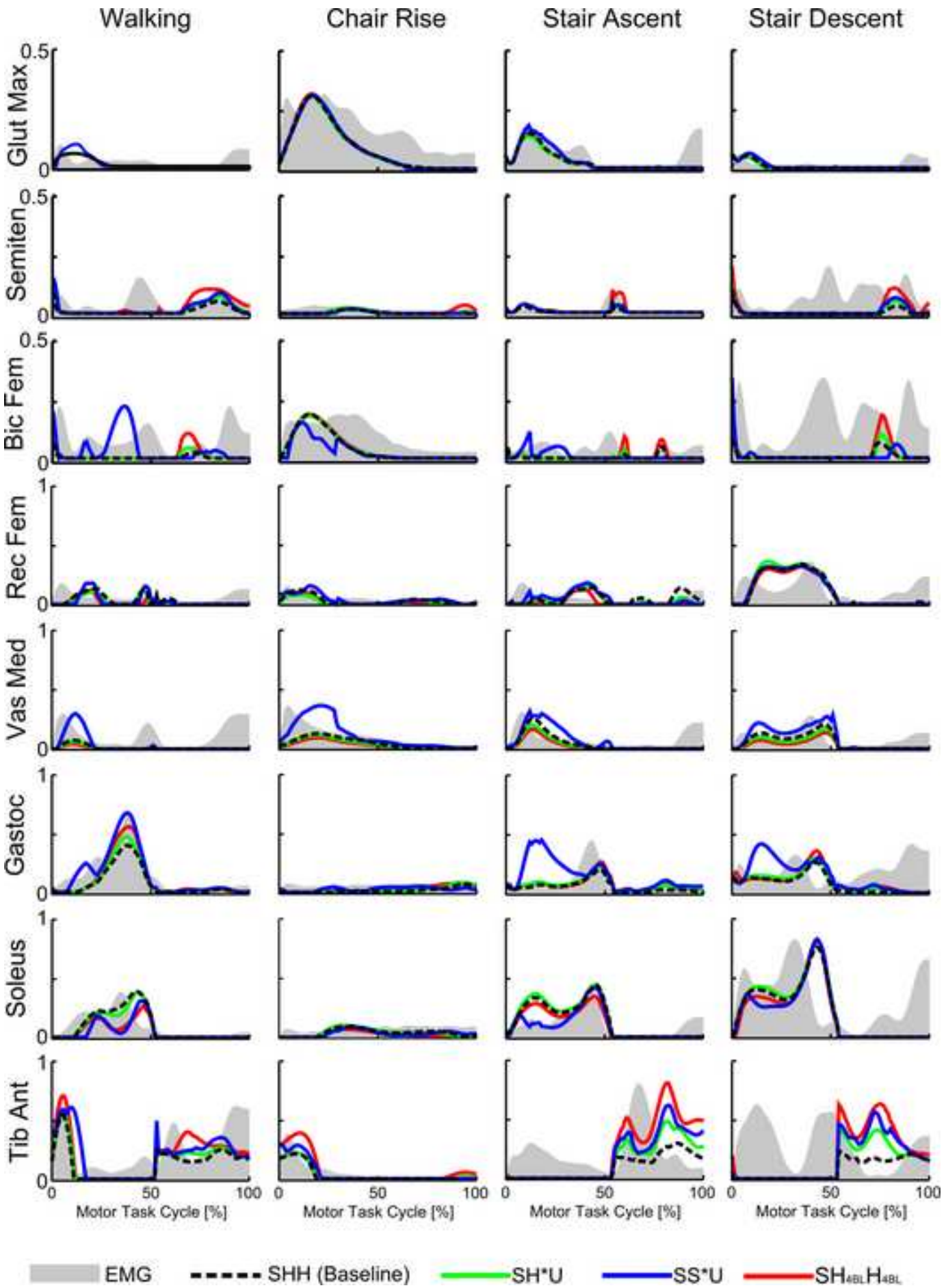


Figure 4

[Click here to download high resolution image](#)

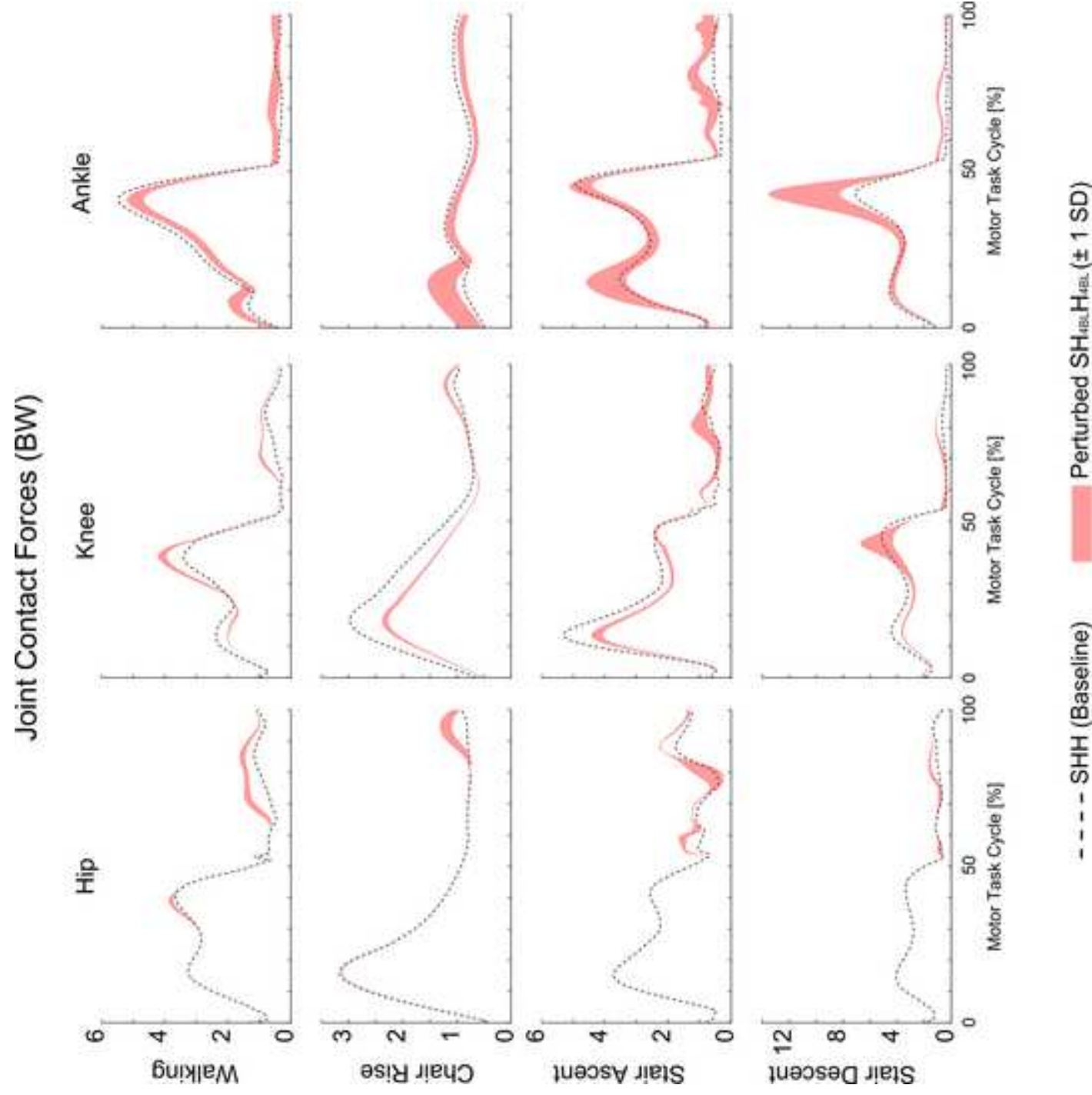


Table 1 Values of the covariance matrix (in mm²) of each ligament landmark position (multivariate normally distributed variables) measured experimentally through virtual palpation on the bone surfaces with the help of the superimposed MRI. The values are reported with the respect to each corresponding body reference frame. The first 3 columns (main diagonal of the covariance matrix) represent the variance along the antero-posterior (x), cranio-caudal (y) and medio-lateral (z) directions of the body reference frames. The last 3 columns (off-diagonal of the covariance matrix) represent the covariance between the couple of elements.

Landmark	x	y	z	xy	xz	yz
ACL origin	1.2	4.0	0.9	-1.0	-0.9	0.4
ACL insertion	2	1.6	0.9	-1.7	-0.3	0.4
PCL origin	2.1	0.9	0.8	-1.1	1.2	-0.6
PCL insertion	1.6	0.6	0.9	0.6	-0.2	0.1
CaFib origin	2.4	6.8	2.1	-2.3	1.6	-3.4
CaFib insertion	2.0	0.7	1.8	0.4	1.1	0.7
TiCal origin	2.3	0.9	1.1	-0.4	-0.3	-0.5
TiCal insertion	11.0	2.9	0.9	-1.5	2.3	-1.0

Table 2

Table 2 Differences in lower-limb joint contact forces between the modified models (SH*U, SS*U, SH_{4BL}H_{4BL}) and the baseline model (SHH) during the four motor tasks simulated. Mean and maximum differences over the motor task cycle are reported in body-weight (BW). Significant differences over the motor task cycle (Wilcoxon signed rank tests ($p < 0.01$)) are highlighted in bold. Pearson correlation coefficients (R) are reported.

	SH*U			SS*U			SH _{4BL} H _{4BL}			
	Hip	Knee	Ankle	Hip	Knee	Ankle	Hip	Knee	Ankle	
Walking	0.06	0.06	0.18	0.31	0.59	0.24	0.20	0.18	-0.05	Mean Diff (BW)
	0.22	0.42	0.51	0.85	2.40	1.31	0.66	1.05	-0.53	Max Diff (BW)
	1.00	0.99	1.00	0.99	0.99	0.99	0.98	0.95	1.00	R
Chair Rise	-0.01	-0.12	0.15	0.23	-0.01	0.16	0.06	-0.21	-0.04	Mean Diff (BW)
	-0.16	-0.42	0.35	0.88	-0.43	0.51	0.50	-0.72	-0.16	Max Diff (BW)
	1.00	0.99	0.88	0.92	0.97	0.77	0.99	0.95	0.84	R
Stair Ascent	0.04	-0.12	0.22	0.22	0.22	0.31	0.13	-0.18	0.07	Mean Diff (BW)
	0.29	-0.71	0.48	1.37	1.21	0.72	0.67	-1.20	0.77	Max Diff (BW)
	0.99	0.99	1.00	0.96	0.98	1.00	0.98	0.98	0.99	R
Stair Descent	0.02	-0.10	0.28	0.08	0.05	0.28	0.11	-0.19	0.25	Mean Diff (BW)
	0.21	-0.57	0.73	0.55	1.07	0.72	0.63	-0.96	1.54	Max Diff (BW)
	1.00	1.00	1.00	0.99	0.97	1.00	0.99	0.99	0.98	R

Table 3 Mean and maximum standard deviations (SD) of lower-limb joint contact forces predicted by the perturbed simulations to study the sensitivity to the uncertainties associated with the creation of the anatomical four-bar linkage at the knee and ankle joints in the SH_{4BL}H_{4BL} model during the four motor tasks. Mean and maximum SD over the motor task cycle are reported in body-weight (BW).

	SH _{4BL} H _{4BL}			
	Hip	Knee	Ankle	
Walking	0.04	0.04	0.16	Mean SD (BW)
	0.15	0.14	0.28	Max SD (BW)
Chair Rise	0.02	0.03	0.10	Mean SD (BW)
	0.11	0.06	0.27	Max SD (BW)
Stair Ascent	0.06	0.10	0.26	Mean SD (BW)
	0.47	0.28	0.66	Max SD (BW)
Stair Descent	0.04	0.17	0.40	Mean SD (BW)
	0.19	1.21	2.66	Max SD (BW)

CONFLICT OF INTEREST STATEMENT

The authors do not have any financial or personal relationships with other people or organization that could inappropriately influence their work.